

PROTEIN FLEXIBILITY AND THE CORRELATION RATCHET*

TIMOTHY C. ELSTON[†], DWIGHT YOU[‡], AND CHARLES S. PESKIN[§]

Abstract. Biomolecular motors are tiny engines that transport material at the microscopic level within biological cells. Since biomolecular motors typically transport cargo that are much larger than themselves, one would expect the speed of such a motor to be severely limited by the small diffusion coefficient of its enormous cargo. It has been suggested by Berg and Kahn [*Mobility and Recognition in Cell Biology*, H. Sund and C. Veeger, eds., De Gruyter, Berlin, 1983] and Meister, Caplan, and Berg [*Biophys. J.*, 55 (1989), pp. 905–914] that this limitation can be overcome if the tether that connects the motor to its cargo is sufficiently elastic. In a recent article the effects of the elastic properties of the tether on the speed of the motor were investigated when the driving mechanism was a Brownian ratchet [*SIAM J. Appl. Math.*, 60 (2000), pp. 842–867]. Here we extend that work to include the correlation ratchet [C. Peskin, G. Ermentrout, and G. Oster, in *Mechanics and Cellular Engineering*, V. Mow et al., eds., Springer, New York, 1994; *Phys. Rev. Lett.*, 72 (1994), pp. 2652–2655; *Phys. Rev. Lett.*, 72 (1994), pp. 1766–1769]. In contrast to the Brownian ratchet, it is shown that in the limit of a large motor diffusion coefficient the average velocity increases monotonically as the stiffness of the tether is increased. However, Monte-Carlo simulations reveal that for any finite diffusion coefficient of the motor there is an optimal stiffness at which the motor travels fastest.

Key words. biomolecular motors, correlation ratchet, protein flexibility, stochastic processes, diffusion equation

AMS subject classification. 92C05

PII. S0036139999353942

1. Introduction. The bacterial flagellar motor (BFM) is a rotary engine used by certain bacteria (e.g., *E. coli*) for motility. The motor runs off a proton gradient maintained across the cell's inner membrane and consists of 8–16 small torque generating elements (stators) that interact with a ring-like structure (the rotor) that in turn spins a large flagellum. It has been suggested by Berg and Kahn [1] and Meister, Caplan, and Berg [2] that the rotation rate of the flagellum can be increased if the linkage connecting the stators to the cell membrane is elastic. In a recent article, two of us (Elston and Peskin) presented an initial investigation into this issue of protein flexibility [3]. In this study the driving mechanism of the motor was a “Brownian” ratchet. It was shown that the motor's speed did indeed increase as the linkage was “softened” and that the benefit obtained in this way depended on two dimensionless quantities: the ratio of the diffusion coefficient of the motor to the diffusion coefficient of the cargo and the ratio of the free energy step at each ratchet site to $k_B T$. However, these conclusions are inconsistent with the behavior shown by the Elston–Oster model of the BFM [7]. In their model the mean velocity decreased as the connecting linkage was softened.

The Elston–Oster model is based on a “correlation” ratchet mechanism [4, 5, 6]. As protons are conducted across the membrane they associate and disassociate with

*Received by the editors March 22, 1999; accepted for publication (in revised form) January 4, 2000; published electronically August 29, 2000. This work was supported by the National Science Foundation under research grant DMS/FD 92-20719.

<http://www.siam.org/journals/siap/61-3/35394.html>

[†]Biomathematics Program, Department of Statistics, North Carolina State University, Raleigh, NC 27695-8203 (elston@stat.ncsu.edu).

[‡]Department of Physics, DePaul University, 2219 Kenmore Ave, Chicago, IL 60614-3504.

[§]Courant Institute of Mathematical Sciences, New York University, 251 Mercer St., New York, NY 10012 (peskin@cims.nyu.edu).

the charged side chains of the channel forming proteins. In doing so, the protons alter the electrostatic potential felt by the rotor and stators. This alternating or “flashing” potential in conjunction with an asymmetric charge distribution on the rotor is sufficient to turn the flagellum [7]. In this article we extend the work of Elston and Peskin to include the correlation ratchet. We show that if the motor’s diffusion coefficient is large enough, then the mean speed of the motor decreases as the linkage is softened, contrary to the behavior of a Brownian ratchet but similar to that of the Elston–Oster model of the BFM. However, we also show by numerical simulation that when the diffusion coefficient of the motor is finite there is an optimal stiffness that maximizes the motor’s speed.

The rest of this article is organized as follows. In section 2, we begin with a description of the problem under consideration. In section 3, the behavior of the motor-cargo system is investigated in three different limiting cases. The different regimes considered are the large motor diffusion coefficient and the stiff and soft spring limits. In section 4 results from a numerical study of the problem are presented. These results serve not only to verify the analysis presented in the previous section, but also reveal new behavior of the system that is not captured by the limiting cases we have been able to analyze. We end with some concluding remarks in section 5.

2. Description of the problem. Figure 2.1 illustrates a small motor pulling a large cargo. The motor is characterized by its diffusion coefficient D_1 and is constrained to move on a one-dimensional (1-D) track positioned along the x direction. Let the position of the motor be denoted by x_1 . The cargo is characterized by its diffusion coefficient D_2 and in general is free to move in three dimensions. However, throughout this article we assume that the linkage connecting the motor and cargo is a linear spring. This has the effect of uncoupling the y and z degrees of freedom and allows the cargo’s position to be described with one spatial coordinate x_2 . The full potential for this problem is

$$(2.1) \quad U(x_1, x_2, t) = \phi(x_1, t) + \frac{1}{2}\kappa(x_1 - x_2)^2,$$

where κ is the spring constant of the tether connecting the motor and cargo and $\phi(x_1, t)$ is the time-dependent ratchet potential that governs the interactions between the motor and track.

As mentioned in the introduction, the motor is driven by a correlation ratchet. That is, $\phi(x_1, t)$ can exist in one of two configurations $\phi_{\pm}(x_1)$, and transitions between these two states occur randomly in time. In the analysis presented below the only assumption made about $\phi_{\pm}(x_1)$ is that each of them is a periodic function of x_1 , with the same period L . This assumption is generally valid for molecular motors, since the tracks on which they move are made from polymers. The repeat interval of the track is typically several nanometers long, similar to characteristic lengths of the motor. If one of the two configurations is spatially asymmetric (i.e., a ratchet potential), then the motor will move with finite average velocity. A simple example that illustrates the correlation ratchet is shown in Figure 2.1. To produce this and all subsequent figures, the following two potentials were used:

$$(2.2) \quad \phi_+(x_1) = \frac{A}{2\pi} \left(\sin\left(\frac{2\pi}{L}x_1\right) - \frac{1}{2}\sin\left(\frac{4\pi}{L}x_1\right) + \frac{1}{3}\sin\left(\frac{6\pi}{L}x_1\right) \right)$$

$$(2.3) \quad \phi_-(x_1) = 0.$$

To understand how this mechanism works note that while in the $+$ -state the motor spends most of its time near the local minima of that potential, and while in the

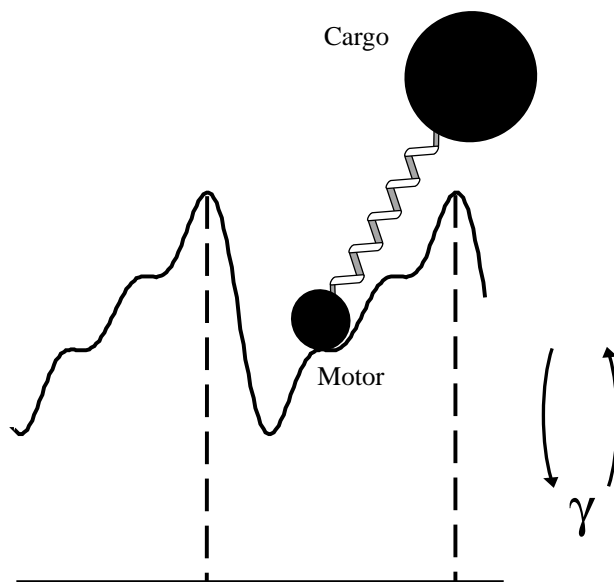


FIG. 2.1. A small motor pulling a large cargo. The motor is driven by a correlation ratchet.

—state the motor is free to diffuse. The two dashed vertical lines in the figure indicate the position of adjacent maxima. Due to the anisotropy of the \pm -potential, when a transition out of the \pm -state occurs the motor is more likely to be located closer to the left vertical line than the right. Therefore, the motor has a greater probability of crossing this boundary. If the motor does cross this boundary and the potential switches back to the \mp -state, the motor will move toward the next potential minima to the left. In this way the motor moves with a net drift to the left.

Let $\rho_{\pm}(x_1, x_2, t)dx_1dx_2$ denote the probability of finding the motor between x_1 and $x_1 + dx_1$, the cargo between x_2 and $x_2 + dx_2$, and the potential to be in the \pm -state at time t . In the overdamped limit, the Fokker-Planck equation that governs ρ_{\pm} is

$$(2.4) \quad \frac{\partial \rho_{\pm}(x_1, x_2, t)}{\partial t} + \frac{\partial J_{1\pm}(x_1, x_2, t)}{\partial x_1} + \frac{\partial J_{2\pm}(x_1, x_2, t)}{\partial x_2} = -\gamma(\rho_{\pm}(x_1, x_2, t) - \rho_{\mp}(x_1, x_2, t)),$$

where γ is the average switching rate and

$$(2.5) \quad J_{1\pm} = -D_1 \left(\frac{\partial \rho_{\pm}}{\partial x_1} + \frac{\rho_{\pm}}{k_B T} \left(\frac{d\phi_{\pm}(x_1)}{dx} + \kappa(x_1 - x_2) \right) \right),$$

$$(2.6) \quad J_{2\pm} = -D_2 \left(\frac{\partial \rho_{\pm}}{\partial x_2} + \frac{\rho_{\pm}}{k_B T} \kappa(x_2 - x_1) \right)$$

are the fluxes for the motor and cargo, respectively. In (2.4) it has been assumed that the intervals between switching times from one state to the other are exponentially distributed. This type of behavior is appropriate if the transitions arise from the

association and dissociation of protons or from the binding and release of ATP. The two transition rates have been taken to be equal. This need not be the case, but we do not expect that the use of different rates would have any qualitative effect on the conclusions of this paper. Equation (2.4) must be solved subject to appropriate boundary and initial conditions. Since the motor and cargo are linked together, they move with the same mean velocity. In the remainder of this article we investigate how this velocity depends on the properties of the connecting spring.

3. Limiting behavior.

3.1. The limit $D_1 \rightarrow \infty$. Following the analysis presented in [3], we first consider the limit in which the diffusion of the motor is a “fast” process. That is, D_1 is large enough to ensure that the motor comes to equilibrium in the potential arising from interactions with the track and cargo before the cargo can move appreciably or the track potential changes state. Letting $D_1 \rightarrow \infty$ in (2.5) yields

$$(3.1) \quad \left(\frac{\partial \rho_{\pm}}{\partial x_1} + \frac{\rho_{\pm}}{k_B T} \left(\frac{d\phi_{\pm}(x_1)}{dx_1} + \kappa(x_1 - x_2) \right) \right) = 0$$

from which it follows that

$$(3.2) \quad \rho_{\pm}(x_1, x_2, t) = \rho_{\pm}^{(0)}(x_2, t) \frac{\exp\left(\frac{-U_{\pm}(x_1, x_2)}{k_B T}\right)}{\int_{-\infty}^{\infty} \exp\left(\frac{-U_{\pm}(x'_1, x_2)}{k_B T}\right) dx'_1},$$

where

$$(3.3) \quad U_{\pm}(x_1, x_2) = \phi_{\pm}(x_1) + \frac{1}{2}\kappa(x_1 - x_2)^2$$

and $\rho_{\pm}^{(0)}(x_2, t)$ is an undetermined function. Using (3.2) in (2.4) and (2.6), it is straightforward to verify that $\rho_{\pm}^{(0)}(x_2, t)$ satisfies the equation

$$(3.4) \quad \frac{\partial \rho_{\pm}^{(0)}(x_2)}{\partial t} + \frac{\partial J_{\pm}^{(0)}(x_2)}{\partial x_2} - \gamma(\rho_{\pm}^{(0)}(x_2) - \rho_{\mp}^{(0)}(x_2)) = 0,$$

where

$$(3.5) \quad J_{\pm}^{(0)}(x_2) = D_2 \left(\frac{\partial \rho_{\pm}^{(0)}}{\partial x_2} + \frac{\rho_{\pm}^{(0)}(x_2)}{k_B T} \frac{d\phi_{\pm}^{(0)}(x_2)}{dx_2} \right).$$

In the above equation, $\phi_{\pm}^{(0)}(x_2)$ represents an “effective potential” or “free energy” felt by the cargo [3] and has the form

$$(3.6) \quad \begin{aligned} \phi_{\pm}^{(0)}(x_2) &= -k_B T \ln \int_{-\infty}^{\infty} \exp\left(-\frac{U_{\pm}(x_1, x_2)}{k_B T}\right) dx_1 \\ &= -k_B T \ln \int_{-\infty}^{\infty} \exp\left(-\frac{\phi_{\pm}(x_1)}{k_B T}\right) \exp\left(-\frac{\frac{1}{2}\kappa(x_1 - x_2)^2}{k_B T}\right) dx_1. \end{aligned}$$

Thus, in the limit of large D_1 the fast degree of freedom associated with the motor can be averaged over, reducing the problem to one of a single spatial dimension.

Let $w_{\pm}(x_1)$ be defined by

$$(3.7) \quad w_{\pm}(x_1) = \exp\left(-\frac{\phi_{\pm}(x_1)}{k_B T}\right).$$

Since w_{\pm} is periodic in x_1 , it makes sense to write it in terms of a Fourier series as was done in [3]. In this case, $\phi_{\pm}^{(0)}$ takes the form

$$(3.8) \quad \phi_{\pm}^{(0)}(x_2) = -k_B T \ln \sum_{n=-\infty}^{\infty} \hat{w}_{\pm n} \exp\left(2\pi i n \frac{x_2}{L} - \frac{2k_B T}{\kappa} \frac{\pi^2}{L^2} n^2\right),$$

where

$$(3.9) \quad \hat{w}_{\pm n} = \frac{1}{L} \int_0^L w_{\pm}(x) \exp\left(-2\pi i \frac{nx}{L}\right) dx.$$

Equation (3.8) can be used to compute the effective potential for any choice of spring constant κ . It has the added advantage of allowing the limiting behavior of $\phi_{\pm}^{(0)}$ to be read off by inspection. The results are

$$(3.10) \quad \begin{aligned} \lim_{\kappa \rightarrow \infty} \phi_{\pm}^{(0)}(x_2) &= -k_B T \ln \sum_{n=-\infty}^{\infty} \hat{w}_{\pm n} \exp\left(2\pi i n \frac{x_2}{L}\right) \\ &= -k_B T \ln w_{\pm}(x_2) \\ &= \phi_{\pm}(x_2) \end{aligned}$$

and

$$(3.11) \quad \begin{aligned} \lim_{\kappa \rightarrow 0} \phi_{\pm}^{(0)}(x_2) &= -k_B T \ln \hat{w}_0 \\ &= \text{constant.} \end{aligned}$$

In the stiff-spring limit the cargo feels the same potential as the motor, but in the soft-spring limit the shape of the potential is lost and the cargo only undergoes diffusion. Thus, in the limit of large D_1 , the velocity of the motor-cargo system goes to zero as the spring is softened. This is to be contrasted with soft-spring limit of the Brownian ratchet in which case the velocity approached a maximum [3].

Using (3.4) and (3.5), an asymptotic expression for the average velocity when $D_1 = \infty$ can be constructed in the limit $\gamma \rightarrow 0$ [4, 8]. The result is

$$(3.12) \quad v = \frac{\gamma L}{2} \int_0^L dx (b_+(x) - b_-(x)) \int_0^x dx' (c_+(x') - c_-(x')),$$

where

$$(3.13) \quad c_{\pm}(x) = \frac{\exp\left(-\frac{\phi_{\pm}^{(0)}(x)}{k_B T}\right)}{\int_0^L dx' \exp\left(-\frac{\phi_{\pm}^{(0)}(x')}{k_B T}\right)},$$

$$(3.14) \quad b_{\pm}(x) = \frac{\exp\left(\frac{\phi_{\pm}^{(0)}(x)}{k_B T}\right)}{\int_0^L dx' \exp\left(\frac{\phi_{\pm}^{(0)}(x')}{k_B T}\right)}.$$

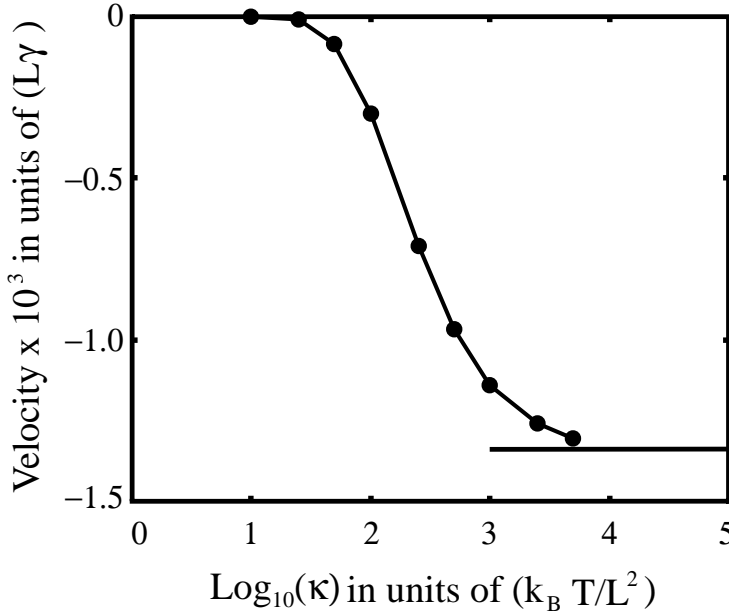


FIG. 3.1. The mean velocity in units of (γL) as a function of $\log_{10}(\kappa)$ for large D_1 and small γ . In this figure $A = 1k_B T$, and the solid line represents the limiting 1-D case.

Note that (3.12) is independent not only of D_1 but also of the diffusion coefficient D_2 of the cargo. This is a result of the assumption that γ is slow enough to allow the cargo to come to equilibrium in the effective potential $\phi_{\pm}^{(0)}$ before a transition occurs. That is, (3.12) is valid when the condition $\gamma^{-1} \ll \frac{L^2}{D_2} \ll \frac{L^2}{D_1}$ is satisfied. In Figure 3.1, (3.12) has been used to generate a plot of the velocity versus the logarithm of the spring constant. The mean velocity starts at zero and monotonically approaches the limiting velocity of a single particle propelled by a correlation ratchet with the potentials ϕ_{\pm} as κ increases. (In the limit under consideration here, the diffusion coefficient of that particle is irrelevant.)

Although (3.12) was derived here by first taking the limit $D_1 \rightarrow \infty$ and then considering small γ (or equivalently, large D_2), we expect that the same result would be obtained by holding γ fixed while simultaneously letting D_1 and D_2 approach ∞ . That is, (3.12) holds when both the motor and cargo have enough time after each change of state to equilibrate with the ambient potential before the next change of state occurs.

3.2. The limit $\kappa \rightarrow \infty$. In the analysis presented above it was assumed that the diffusion coefficient of the motor was large enough to ensure that the motor came to thermal equilibrium before the potential switched states or the cargo could move appreciably. In this section we allow the diffusion coefficient of the motor to remain finite and investigate the limit $\kappa \rightarrow \infty$.

A natural choice of dimensionless variables for this problem is [3]

$$(3.15) \quad x = \frac{x_1}{L},$$

$$(3.16) \quad y = \sqrt{\frac{\kappa}{k_B T}}(x_2 - x_1),$$

$$(3.17) \quad s = \frac{D_1}{L^2}t.$$

Noting that

$$(3.18) \quad \frac{\partial(x, y)}{\partial(x_1, x_2)} = \frac{1}{L} \sqrt{\frac{\kappa}{k_B T}},$$

let $\sigma_{\pm}(x, y)$ be defined by

$$(3.19) \quad \begin{aligned} \rho_{\pm}(x_1)dx_1dx_2 &= \sigma_{\pm}(x, y)dxdy \\ &= \sigma_{\pm}\left(\frac{x_1}{L}, \sqrt{\frac{\kappa}{k_B T}}(x_2 - x_1)\right) \left(\frac{1}{L} \sqrt{\frac{\kappa}{k_B T}}\right) dx_1dx_2. \end{aligned}$$

In terms of the dimensionless variables, the equation satisfied by σ_{\pm} is

$$(3.20) \quad \begin{aligned} \frac{\partial\sigma_{\pm}}{\partial s} &= \frac{\partial}{\partial x} \left[\frac{\partial}{\partial x} \sigma_{\pm} + \sigma_{\pm} \frac{d\phi'}{dx} \right] - \gamma' \sigma_{\pm} + \gamma' \sigma_{\mp} \\ &\quad - \beta \left[\frac{\partial}{\partial x} \left(\frac{\partial\sigma_{\pm}}{\partial y} + y\sigma_{\pm} \right) + \frac{\partial}{\partial y} \left(\frac{\partial\sigma_{\pm}}{\partial x} + \sigma_{\pm} \frac{d\phi'}{dx} \right) \right] \\ &\quad + \beta^2(1 + \epsilon) \frac{\partial}{\partial y} \left[\frac{\partial\sigma_{\pm}}{\partial y} + y\sigma_{\pm} \right]. \end{aligned}$$

The dimensionless parameters appearing in the above equation are defined as follows:

$$(3.21) \quad \beta = L \sqrt{\frac{\kappa}{k_B T}}, \quad \epsilon = \frac{D_2}{D_1},$$

$$(3.22) \quad \phi' = \frac{\phi}{k_B T}, \quad \gamma' = \frac{L^2}{D_1} \gamma.$$

To investigate the $\kappa \rightarrow \infty$ limit ($\beta \rightarrow \infty$), rewrite (3.20) in the form

$$(3.23) \quad \begin{aligned} (1 + \epsilon) \frac{\partial}{\partial y} \left[\frac{\partial\sigma_{\pm}}{\partial y} + y\sigma_{\pm} \right] &= \frac{1}{\beta} \left[\frac{\partial}{\partial x} \left(\frac{\partial\sigma_{\pm}}{\partial y} + y\sigma_{\pm} \right) + \frac{\partial}{\partial y} \left(\frac{\partial\sigma_{\pm}}{\partial x} + \sigma_{\pm} \frac{d\phi'_{\pm}}{dx} \right) \right] \\ &\quad + \frac{1}{\beta^2} \left[\frac{\partial\sigma_{\pm}}{\partial s} - \frac{\partial}{\partial x} \left[\frac{\partial}{\partial x} \sigma_{\pm} + \sigma_{\pm} \frac{d\phi'_{\pm}}{dx} \right] - \gamma' \sigma_{\pm} + \gamma' \sigma_{\mp} \right]. \end{aligned}$$

A power series expansion in terms of $\frac{1}{\beta}$ for σ_{\pm} is

$$(3.24) \quad \sigma_{\pm} = \sigma_{\pm}^{(0)} + \frac{1}{\beta} \sigma_{\pm}^{(1)} + \frac{1}{\beta^2} \sigma_{\pm}^{(2)} + \dots$$

The first three terms in the above expansion satisfy the following equations:

$$(3.25) \quad \begin{aligned} (1 + \epsilon) \frac{\partial}{\partial y} \left[\frac{\partial\sigma_{\pm}^{(0)}}{\partial y} + y\sigma_{\pm}^{(0)} \right] &= 0, \\ (1 + \epsilon) \frac{\partial}{\partial y} \left[\frac{\partial\sigma_{\pm}^{(1)}}{\partial y} + y\sigma_{\pm}^{(1)} \right] &= \frac{\partial}{\partial x} \left(\frac{\partial\sigma_{\pm}^{(0)}}{\partial y} + y\sigma_{\pm}^{(0)} \right) \end{aligned}$$

$$\begin{aligned}
 (3.26) \quad & + \frac{\partial}{\partial y} \left(\frac{\partial \sigma_{\pm}^{(0)}}{\partial x} + \sigma_{\pm}^{(0)} \frac{d\phi'_{\pm}}{dx} \right), \\
 (1 + \epsilon) \frac{\partial}{\partial y} \left[\frac{\partial \sigma_{\pm}^{(2)}}{\partial y} + y \sigma_{\pm}^{(2)} \right] &= \frac{\partial}{\partial x} \left(\frac{\partial \sigma_{\pm}^{(1)}}{\partial y} + y \sigma_{\pm}^{(1)} \right) \\
 & + \frac{\partial}{\partial y} \left(\frac{\partial \sigma_{\pm}^{(1)}}{\partial x} + \sigma_{\pm}^{(1)} \frac{d\phi'_{\pm}}{dx} \right) \\
 & + \frac{\partial \sigma_{\pm}^{(0)}}{\partial s} - \frac{\partial}{\partial x} \left(\frac{\partial \sigma_{\pm}^{(0)}}{\partial x} + \sigma_{\pm}^{(0)} \frac{d\phi'_{\pm}}{dx} \right) \\
 (3.27) \quad & - \gamma' (\sigma_{\pm}^{(0)} - \sigma_{\mp}^{(0)}).
 \end{aligned}$$

To make further progress, it is convenient to introduce the eigenfunctions $R_n(y)$ defined by the equation [8]

$$(3.28) \quad \frac{\partial}{\partial y} \left(\frac{\partial}{\partial y} + y \right) R_n(y) = -n R_n(y).$$

The $R_n(y)$ can be written in the form

$$(3.29) \quad R_n(y) = H_n(y) \frac{e^{-\frac{y^2}{2}}}{\sqrt{2\pi}},$$

where the Hermite polynomials $H_n(y)$ are defined by

$$(3.30) \quad H_n(y) = (-1)^n e^{\frac{y^2}{2}} \frac{d^n}{dy^n} e^{-\frac{y^2}{2}}.$$

The following analysis makes use of the two identities:

$$(3.31) \quad y R_n = R_{n+1} + n R_{n-1},$$

$$(3.32) \quad \frac{dR_n}{dy} = -R_{n+1}.$$

Equations (3.25)–(3.27) can now be used to construct an equation that governs the dynamics of the motor-cargo system in the stiff-spring limit. Solving (3.25) for $\sigma_{\pm}^{(0)}$ yields

$$(3.33) \quad \sigma_{\pm}^{(0)}(x, y, s) = f_{\pm}^{(0)}(x, s) R_0(y),$$

where $f_{\pm}^{(0)}(x, s)$ is an undetermined function of the dimensionless variables x and s . To get a condition on $f_{\pm}^{(0)}$, use is made of the higher-order terms in the expansion of σ_{\pm} . Substituting (3.33) into (3.26) and making use of (3.31) and (3.32) allows the $\frac{1}{\beta}$ -equation to be written as

$$(3.34) \quad \frac{\partial}{\partial y} \left[\frac{\partial \sigma_{\pm}^{(1)}}{\partial y} + y \sigma_{\pm}^{(1)} \right] = -\frac{1}{(1 + \epsilon)} \left(\frac{\partial f_{\pm}^{(0)}}{\partial x} + f_{\pm}^{(0)} \frac{d\phi'_{\pm}}{dx} \right) R_1.$$

Equation (3.34) together with (3.28) imply that $\sigma_{\pm}^{(1)}$ has the form

$$(3.35) \quad \sigma_{\pm}^{(1)} = \frac{1}{(1 + \epsilon)} \left(\frac{\partial f_{\pm}^{(0)}}{\partial x} + f_{\pm}^{(0)} \frac{d\phi'_{\pm}}{dx} \right) R_1 + f_{\pm}^{(1)} R^{(0)},$$

where $f_{\pm}^{(1)}$ is an undetermined function of x and s . Substituting (3.33) and (3.35) into (3.27) and again making use of (3.31) and (3.32) produces the result

$$(1 + \epsilon) \frac{\partial}{\partial y} \left[\frac{\partial \sigma_{\pm}^{(2)}}{\partial y} + y \sigma_{\pm}^{(2)} \right] = \left\{ \frac{1}{(1 + \epsilon)} \left(\frac{\partial f_{\pm}^{(0)}}{\partial x} + f_{\pm}^{(0)} \frac{d\phi'_{\pm}}{dx} \right) + \frac{\partial f_{\pm}^{(0)}}{\partial s} - \frac{\partial}{\partial x} \left(\frac{\partial f_{\pm}^{(0)}}{\partial x} + f_{\pm}^{(0)} \frac{d\phi'_{\pm}}{dx} \right) - \gamma'(f_{\pm}^{(0)} - f_{\mp}^{(0)}) \right\} R_0$$

(3.36) + terms involving R_1 and R_2 .

Since R_0 has a zero eigenvalue, the coefficient multiplying it in the above equation must vanish. This means $f_{\pm}^{(0)}$ satisfies the equation

$$(3.37) \quad \frac{\partial f_{\pm}^{(0)}}{\partial s} - \frac{\epsilon}{1 + \epsilon} \frac{\partial}{\partial x} \left(\frac{\partial f_{\pm}^{(0)}}{\partial x} + f_{\pm}^{(0)} \frac{d\phi'_{\pm}}{dx} \right) - \gamma'(f_{\pm}^{(0)} - f_{\mp}^{(0)}) = 0.$$

If we now convert back to the unscaled variables, the equation governing $f_{\pm}^{(0)}$ becomes

$$(3.38) \quad \frac{\partial f_{\pm}^{(0)}}{\partial t} - \frac{D_1 D_2}{D_1 + D_2} \frac{\partial}{\partial x_1} \left(\frac{\partial f_{\pm}^{(0)}}{\partial x_1} + \frac{f_{\pm}^{(0)}}{k_B T} \frac{d\phi_{\pm}}{dx_1} \right) - \gamma(f_{\pm}^{(0)} - f_{\mp}^{(0)}) = 0.$$

This is the equation of a 1-D correlation ratchet. Thus, in the limit $\kappa \rightarrow \infty$, the dynamics of the system reduces to that of a single particle with an effective diffusion coefficient $D_{\text{eff}} = \frac{D_1 D_2}{D_1 + D_2}$.

3.3. The limit $\kappa \rightarrow 0$. Next consider the opposite limit $\kappa \rightarrow 0$ ($\beta \rightarrow 0$). To study this case introduce the scaling $z = \beta y$ [3] and let $\tau_{\pm}(x, z)$ be defined by

$$(3.39) \quad \sigma_{\pm}(x, y) dx dy = \tau_{\pm}(x, \beta y) dx \beta dy.$$

Making these changes in (3.20) leads to the following equation for τ_{\pm} :

$$(3.40) \quad \begin{aligned} \frac{\partial \tau_{\pm}}{\partial s} &= \frac{\partial}{\partial x} \left[\frac{\partial}{\partial x} \tau_{\pm} + \tau_{\pm} \left(\frac{d\phi'_{\pm}}{dx} - z \right) \right] - \gamma' \tau_{\pm} + \gamma' \tau_{\mp} \\ &\quad - \beta^2 \frac{\partial}{\partial z} \left[2 \frac{\partial \tau_{\pm}}{\partial x} + \tau_{\pm} \left(\frac{d\phi'_{\pm}}{dx} - (1 + \epsilon) z \right) \right] \\ &\quad + \beta^4 (1 + \epsilon) \frac{\partial^2 \tau_{\pm}}{\partial z^2}. \end{aligned}$$

In this limit we only consider the steady-state properties of the system. That is, the left-hand side of (3.40) is set equal to zero. The boundary and normalization conditions are then given by

$$(3.41) \quad \tau_{\pm}(x + 1, z) = \tau_{\pm}(x, z),$$

$$(3.42) \quad \int_{-\infty}^{\infty} dz \int_0^1 dx (\tau_+ + \tau_-) = 1,$$

and it is assumed that $\tau_{\pm} \rightarrow 0$ as $|z| \rightarrow \infty$ for all finite x . Since only even powers of β appear in (3.40), it is reasonable to expand τ_{\pm} in the power series

$$(3.43) \quad \tau_{\pm}(x, z, \beta) = \tau_{\pm}^{(0)}(x, z) + \beta^2 \tau_{\pm}^{(2)}(x, z) + \dots$$

To lowest order in β we have

$$(3.44) \quad 0 = \frac{\partial}{\partial x} \left[\frac{\partial}{\partial x} \tau_{\pm}^{(0)} + \tau_{\pm}^{(0)} \left(\frac{d\phi'_{\pm}}{dx} - z \right) \right] - \gamma' \tau_{\pm}^{(0)} + \gamma' \tau_{\mp}^{(0)}.$$

The above equation has a simple physical interpretation. It is the equation for a correlation ratchet subjected to a “constant” force z . In general analytic solutions to this equation cannot be found. However, we can write the solution symbolically as

$$(3.45) \quad \tau_{\pm}^{(0)} = \frac{f(z) g_{\pm}^{(0)}(x, z)}{2 Z_{\pm}(z)},$$

where $\frac{g_{\pm}^{(0)}(x, z)}{Z_{\pm}(z)}$ satisfies (3.44) and

$$(3.46) \quad Z_{\pm}(z) = \int_0^1 g_{\pm}^{(0)}(x, z) dx.$$

Note that

$$(3.47) \quad \frac{1}{2} \int_0^1 \left(\frac{g_+^{(0)}(x, z)}{Z_+(z)} + \frac{g_-^{(0)}(x, z)}{Z_-(z)} \right) dx = 1$$

and

$$(3.48) \quad \frac{g_{\pm}^{(0)}(x, z)}{Z_{\pm}(z)} \geq 0$$

for all z , since $\frac{g_{\pm}^{(0)}(x, z)}{Z_{\pm}(z)}$ can be interpreted as a probability density. From these two observations it follows that $f(z)$ satisfies the following two properties:

$$(3.49) \quad f(z) \geq 0,$$

$$(3.50) \quad \int_{-\infty}^{\infty} f(z) dz = 1.$$

The β^2 equation is

$$(3.51) \quad \begin{aligned} & \frac{\partial}{\partial x} \left[\frac{\partial}{\partial x} \tau_{\pm}^{(2)} + \tau_{\pm}^{(2)} \left(\frac{d\phi'_{\pm}}{dx} - z \right) \right] - \gamma' \tau_{\pm}^{(2)} + \gamma' \tau_{\mp}^{(2)} \\ & = \frac{\partial}{\partial z} \left[2 \frac{\partial \tau_{\pm}^{(0)}}{\partial x} + \tau_{\pm}^{(0)} \left(\frac{d\phi'_{\pm}}{dx} - (1 + \epsilon)z \right) \right]. \end{aligned}$$

Integrating both sides of (3.51) with respect to x over the interval $(0, 1)$ and making use of the periodic boundary condition yields

$$(3.52) \quad -\gamma' \int_0^1 (\tau_{\pm}^{(2)} - \tau_{\mp}^{(2)}) dx = \frac{\partial}{\partial z} \int_0^1 \tau_{\pm}^{(0)} \left(\frac{d\phi'_{\pm}}{dx} - (1 + \epsilon)z \right) dx.$$

If the above + and - equations are added together, the left-hand sides of these equations cancel. This implies that $\tau_+^{(0)}$ and $\tau_-^{(0)}$ satisfy the relation

$$(3.53) \quad 0 = \frac{\partial}{\partial z} \int_0^1 dx \left[\tau_+^{(0)} \left(\frac{d\phi'_+}{dx} - (1 + \epsilon)z \right) + \tau_-^{(0)} \left(\frac{d\phi'_-}{dx} - (1 + \epsilon)z \right) \right].$$

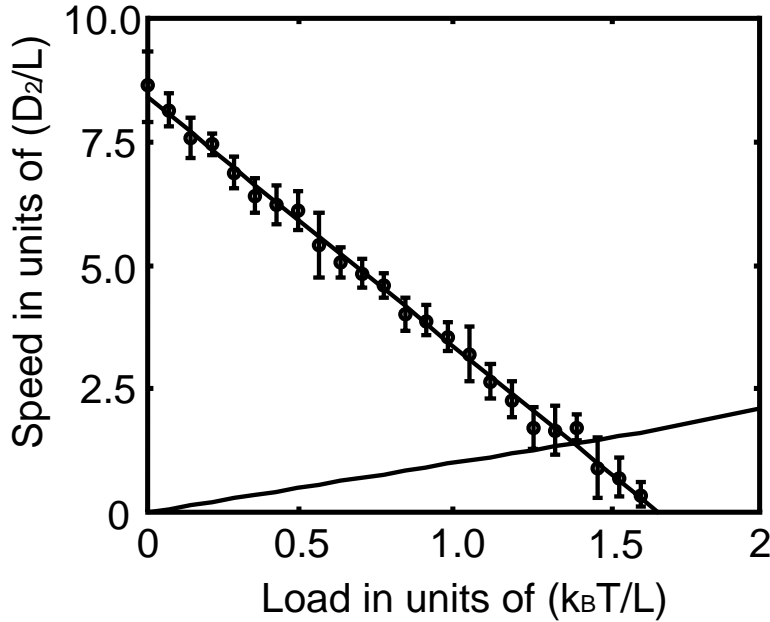


FIG. 3.2. A load-velocity plot for the motor. The speed of the motor is plotted in units of (D_2/L) . In this figure $\epsilon = .1$, $\gamma = 10D_2/L^2$ and $A = 37.5k_B T$. The intersection of the load-velocity curve and the load-line is the average speed of the system in the limit $\kappa \rightarrow 0$.

To simplify the notation, we introduce the following definition:

$$(3.54) \quad \left\langle -\frac{d\phi'_\pm}{dx} + z \right\rangle_\pm = \int_0^1 dx \frac{g_\pm^{(0)}(x, z)}{Z_\pm(z)} \left(-\frac{d\phi'_\pm}{dx} + z \right).$$

Using this definition in (3.53) and integrating with respect to z produces the result

$$(3.55) \quad C = -f(z) \left[\frac{1}{2} \left(\left\langle -\frac{d\phi'_+}{dx} + z \right\rangle_+ + \left\langle -\frac{d\phi'_-}{dx} + z \right\rangle_- \right) + \epsilon z \right],$$

where use has been made of (3.45) and C is an integration constant. Note that the first term inside the square brackets on the right-hand side of (3.55) is the average velocity of a correlation ratchet subjected to a constant load force z . Therefore, this term increases monotonically with z . In fact the entire quantity within the square brackets is a monotonically increasing function of z and ranges from $-\infty$ to ∞ . That is, there exists a unique value z_0 for which this quantity is zero. Since C is a constant (and cannot change sign) and $f(z)$ must satisfy properties (3.49) and (3.50), the only possibility for $f(z)$ is

$$(3.56) \quad f(z) = \delta(z - z_0),$$

where z_0 is determined from the equation

$$(3.57) \quad \frac{1}{2} \left(\left\langle -\frac{d\phi'_+}{dx} + z_0 \right\rangle_+ + \left\langle -\frac{d\phi'_-}{dx} + z_0 \right\rangle_- \right) = -\epsilon z_0.$$

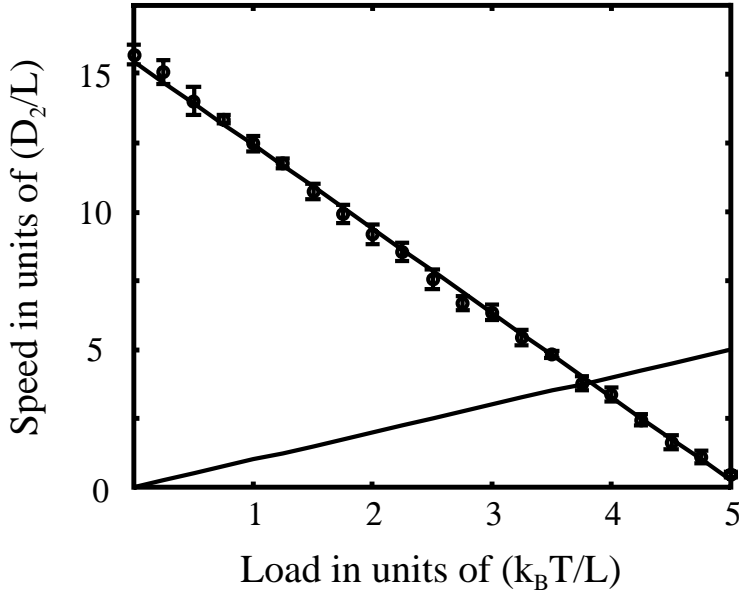


FIG. 3.3. Same as Figure 3.2 except $\gamma = 100D_2/L^2$.

If we make the association $z_0 = -\frac{FL}{k_B T}$, where F has the units of force, and convert back to the unscaled variables (3.57) can be written as

$$\begin{aligned}
 \frac{D_2}{k_B T} F &= \frac{D_1}{k_B T} \frac{1}{2} \left(\left\langle -\frac{d\phi_+}{dx} - F \right\rangle_+ + \left\langle -\frac{d\phi_-}{dx} - F \right\rangle_- \right) \\
 (3.58) \qquad &= v_1(-F),
 \end{aligned}$$

where v_1 is the average velocity of the motor as a function of the an applied load of force F . Equation (3.58) has a simple physical interpretation. In the soft-spring limit, the cargo trails far behind the motor. The net effect of the cargo is then to supply a constant load force on the motor in the opposite direction of the motor’s average velocity. From Newton’s third law we know that the motor must exert an equal and opposite force on the cargo, and this force must be sufficient to keep the cargo moving at the same speed as the motor.

Figures 3.2 and 3.3 give graphical representations of (3.58). Plotted in these figures are load-velocity curves for the motor. To simplify the graphs, we have actually plotted the motor’s speed ($|v|$) as a function of an opposing load force. The data points are the results of Monte-Carlo simulations (the details of which are given in the next section), and the solid line represents a linear fit to the data. Also plotted are load-lines for the cargo. The load force has been measured in units of $k_B T/L$, which means the slope of the load-lines is 1. The point at which two lines intersects represents the average velocity of the system in the limit $\kappa \rightarrow 0$. These results are compared with numerical simulations of the full problem in the next section.

4. Numerical results. In this section we present a numerical investigation of the problem. This serves not only to verify the results of the analysis presented above,

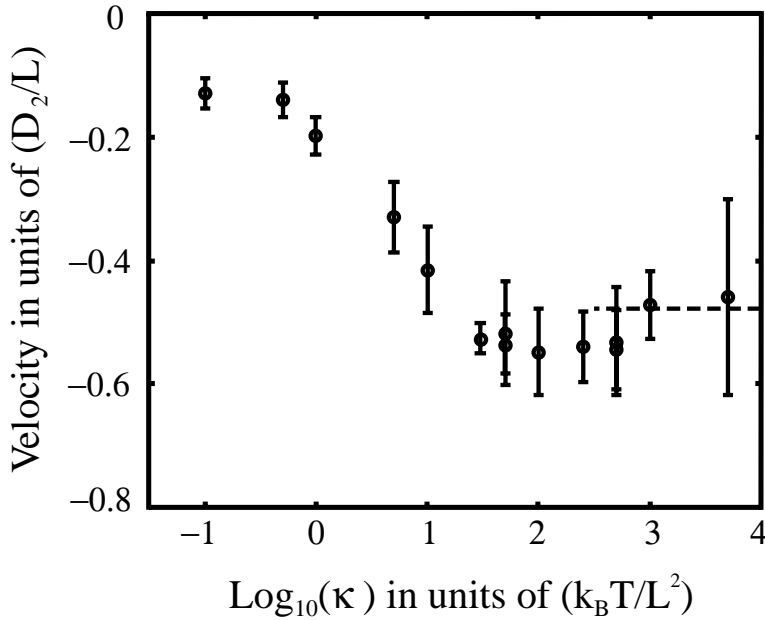


FIG. 4.1. The velocity as a function of $\log_{10}(\kappa)$. The spring constant has units of $(k_B T/L^2)$. In this figure $\epsilon = .1$, $\gamma = .1D_2/L^2$, and $A = 37.5k_B T$. The dashed vertical line represents the average velocity in the limit $\kappa \rightarrow \infty$.

but also allows us to study the dynamics of system away from the limiting cases thus far considered. To simulate the dynamics described by (2.4), use was made of the associated Langevin equations for the motor and cargo:

$$(4.1) \quad \dot{x}_1 = -\frac{D_1}{k_B T} \frac{\partial U(x_1, x_2, t)}{\partial x_1} + \tilde{f}_1(t),$$

$$(4.2) \quad \dot{x}_2 = -\frac{D_2}{k_B T} \frac{\partial U(x_1, x_2, t)}{\partial x_2} + \tilde{f}_2(t),$$

where \tilde{f}_1 and \tilde{f}_2 are Gaussian white noise terms characterized by

$$(4.3) \quad \langle f_i(t) \rangle = 0,$$

$$(4.4) \quad \langle f_i(t) f_j(s) \rangle = 2D_i \delta(t-s) \delta_{ij}.$$

The numerical scheme used to simulate the equations was the standard Euler method for stochastic differential equations. Figures 4.1–4.3 are plots of the mean velocity versus the log of the spring constant κ for various parameter values. In all three of these figures the numerics were carried out in three different stages. For $\kappa \leq 50k_B T/L^2$, (4.1) and (4.2) were directly simulated with a step size of $dt = 5 \times 10^{-4} L^2/D_2$. For larger values of κ the following dimensionless variables were used:

$$(4.5) \quad x'_1 = \sqrt{\frac{\kappa}{k_B T}} x_1, \quad x'_2 = \sqrt{\frac{\kappa}{k_B T}} x_2, \quad t' = \frac{\kappa D_1}{k_B T} t.$$

The large κ values were then further divided in to two groups. For values of κ in the range $50k_B T/L^2 \leq \kappa \leq 500k_B T/L^2$, the dimensionless time step was taken to be .01,

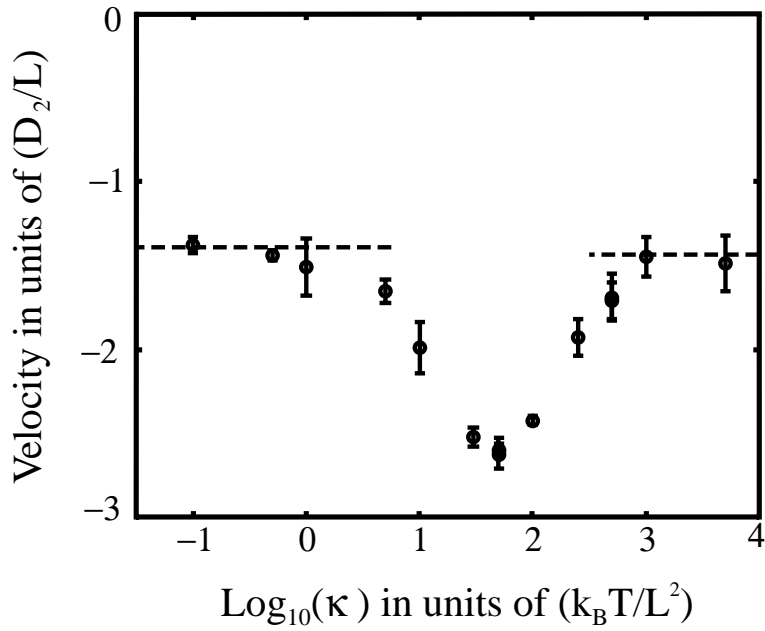


FIG. 4.2. The velocity as a function of $\log_{10}(\kappa)$. The parameters used to produce this plot are the same as in Figure 3.2. The dashed vertical lines represent the average velocity in the limits $\kappa \rightarrow 0$ and $\kappa \rightarrow \infty$.

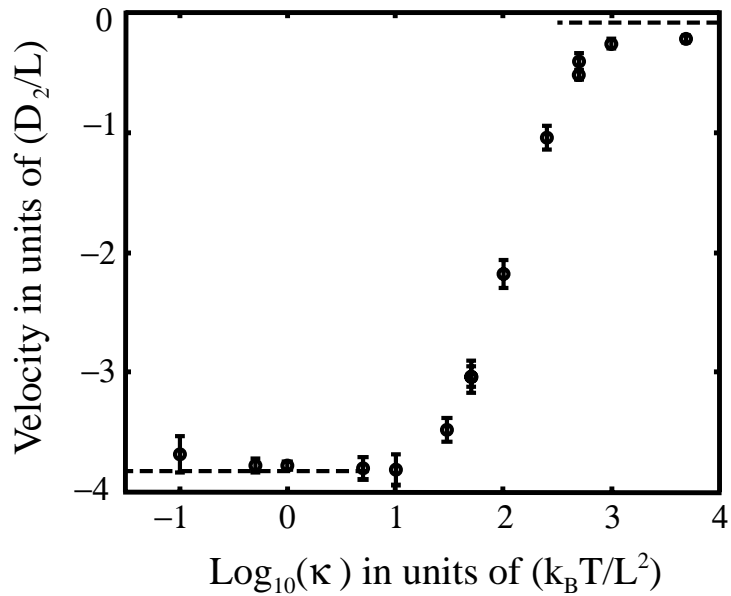


FIG. 4.3. Same as Figure 4.2 except with the parameters used in Figure 3.3.

and for values of κ greater than $500k_B T/L^2$, the dimensionless time step used in the simulations was 5×10^{-3} . As a check on the numerics, the points at the boundaries of the three regions were computed using the two corresponding methods. Each data point listed represents the average of 25 realizations of the process and the width of the error bars is four times the standard error due to finite sampling. To compute the $\kappa \rightarrow \infty$ limiting value shown in these figures, the unscaled version of (4.1) was used with $\kappa = 0$, $\epsilon = 0.1$, $dt = 5 \times 10^{-4} L^2/D_1$, and D_1 taken to be $D_{\text{eff}} = D_2/(1 + \epsilon)$. Similarly the load-velocity plots shown in Figures 3.1 and 3.2 were generated by using (4.1) with κ equal to zero. However, for this case a constant force term was added to (4.1), and the value of D_1 was that of the motor's diffusion coefficient.

In section 3 it was shown that in the limit of large motor diffusion coefficient the mean velocity of the system monotonically decreases as the spring connecting the motor and cargo is softened. In this limit the cargo moves in an effective potential given by (3.6). It was also shown that if the further assumption $\gamma \ll D_2/L^2$ is made, then an asymptotic expression for the mean velocity can be constructed. The results of these considerations are shown in Figure 3.1. It is computationally prohibitive to achieve quantitative agreement between the asymptotic result and Monte-Carlo simulations, since in this limit the average velocity is very small and the variance of the velocity is large. However, in the limit of large D_1 we expect the velocity to monotonically increase with κ for all values of γ , since the effect of softening the spring is to wash out the details of ϕ_{\pm} . Figure 4.1 shows results from Monte-Carlo simulations with $\epsilon = D_2/D_1 = .1$, $\gamma = .1D_2/L^2$, and $A = 37.5k_B T$. The dashed horizontal line represents the numerically calculated average velocity in the stiff-spring limit. That is, the 1-D case with $D_{\text{eff}} = D_2/(1 + \epsilon)$. The results are qualitatively similar to those shown in Figure 3.1 with the velocity decreasing as the spring is softened. However, there is an indication that the curve passes through a maximum as κ is varied. This appearance of an extremum is not inconsistent with the large D_1 result, since in the simulations a finite value of D_1 was used.

To further investigate the existence of an optimal value of κ , simulations were carried out with γ equal to $10D_2/L^2$ and $100D_2/L^2$. The results are shown in Figures 4.2 and 4.3. In these figures the dashed horizontal lines on the right-hand side again represent the stiff-spring limit found from numerical simulations of the corresponding 1-D case. The dashed horizontal lines on the left-hand side represent the soft-spring limit; i.e., the point of intersection of the load-velocity curve and the load-lines plotted in Figures 3.1 and 3.2. The good agreement between the numerics and the limiting cases provides an additional check of the numerics. The $\gamma = 10D_2/L^2$ case clearly shows an extremum. The mean speed is fastest when κ is around $50k_B T/L^2$. For $\gamma = 100D_2/L^2$ the existence of an optimal κ is not so clear. However, it is interesting to note that in this case the mean speed in the soft-spring limit is faster than in the stiff-spring limit. In general a finite value of κ exists for which the system travels fastest, and whether the speed is faster in the stiff- or soft-spring limit depends on the values of D_1 and γ .

5. Conclusions. The correlation ratchet has been suggested as an operating principle for various biomolecular motors [4, 6, 7]. In particular Elston and Oster have shown that a model for the BFM based on this principle is capable of reproducing the observed mechanical properties of the motor. They also showed numerically that as the linkage connecting the motor and cargo was softened, the average velocity decreased. This behavior is exactly opposite to the behavior displayed by the Brownian ratchet [3], in which the average velocity increases as the linkage is softened. The key

difference between the correlation ratchet and the Brownian ratchet is that for the correlation ratchet at any instant of time, the spatial average of the forces arising from the motor-track interaction is zero, whereas the Brownian ratchet experiences a drop in potential energy each time a ratchet barrier is crossed. In the limit of large motor diffusion coefficient, the relevant limit for the BFM, as the linkage connecting the motor and cargo is softened the small scale details of the motor-track potential are washed out. The important feature of the potential is its average slope. Since the slope is zero in both configurations of the correlation ratchet, the cargo effectively undergoes pure diffusion. Thus, the average velocity goes to zero.

For the Brownian ratchet it was found that in general the mean velocity of the motor-cargo system decreased monotonically as the linkage was stiffened [3]. The correlation ratchet involves an additional time scale, namely, the average switching rate. Therefore, we expect the dynamics of this system to be more complex. Indeed, for finite values of D_1 the mean speed goes through a maximum as the spring constant is varied. And the relationship between the average velocity in the soft and stiff spring limits is determined by the values of D_1 and γ .

The correlation ratchet and Brownian ratchet are not mutually exclusive operating principles, and it is conceivable that actual biomolecular motors use a combination of these mechanisms (or neither). However, since biomolecular motors tend to function in the regime where the fastest time scale is set by the diffusion coefficient of the motor, the two models make opposite predictions. If the driving mechanism were indeed based on a correlation ratchet, then one would expect to find the protein linkage connecting the motor and cargo to be stiff. Indeed, given the other parameters of a correlation ratchet, one can calculate the optimal stiffness of the linkage, and this can be compared to the actual stiffness as measured in a laser trap [9]. On the other hand, if a biomolecular motor operates primarily by a Brownian ratchet mechanism, one would expect to find a soft linkage between the motor and its cargo.

Acknowledgments. The authors would like to thank C. R. Doering and G. Oster for stimulating conversations.

REFERENCES

- [1] H. BERG AND S. KAHN, *A model for the flagellar rotary motor*, in *Mobility and Recognition in Cell Biology*, H. Sund and C. Veeger, eds., de Gruyter, Berlin, 1983, pp. 485–497.
- [2] M. MEISTER, S. R. CAPLAN, AND H. BERG, *Dynamics of a tightly coupled mechanism for flagellar rotation*, *Biophys. J.*, 55 (1989), pp. 905–914.
- [3] T. ELSTON AND C. PESKIN, *The role of protein flexibility in molecular motor function: Coupled diffusion in a tilted periodic potential*, *SIAM J. Appl. Math.*, 60 (2000), pp. 842–867.
- [4] C. PESKIN, G. ERMENTROUT, AND G. OSTER, *The correlation ratchet, a novel mechanism for generating directed motion by ATP hydrolysis*, in *Mechanics and Cellular Engineering*, V. Mow, et al., eds., Springer, New York, 1994, pp. 479–489.
- [5] J. PROST, J.-F. CHAUWIN, L. PELITI, AND A. AJDARI, *Assymetric pumping of particles*, *Phys. Rev. Lett.*, 72 (1994), pp. 2652–2655.
- [6] R. ASTUMIAN AND M. BIER, *Fluctuation driven ratchet: Molecular motor*, *Phys. Rev. Lett.*, 72 (1994), pp. 1766–1769.
- [7] T. C. ELSTON AND G. OSTER, *Protein turbines I: The bacterial flagellar motor*, *Biophys. J.*, 73 (1997), pp. 703–721.
- [8] C. DOERING, *Modeling complex systems: Stochastic processes, stochastic differential equations, and Fokker–Planck equations*, in *1990 Lectures in Complex Systems*, L. Nadel and D. Stein, eds., SFI Studies in the Sciences of Complexity, Addison-Wesley, Reading, MA, 1991.
- [9] K. SVOBODA AND S. BLOCK, *Fifty ways to love your lever: Myosin motors*, *Cell*, 77 (1994), pp. 773–784.